Journal of Experimental Marine Biology and Ecology 410 (2011) 61–71

Contents lists available at SciVerse ScienceDirect

Journal of Experimental Marine Biology and Ecology

journal homepage: www.elsevier.com/locate/jembe

Biogeochemical response of *Emiliania huxleyi* (PML B92/11) to elevated CO_2 and temperature under phosphorous limitation: A chemostat study

Corinna Borchard [a], Alberto V. Borges [b], Nicole Händel [a], Anja Engel [c,*]

[a] *Alfred Wegener Institute for Polar and Marine Research, Am Handelshafen 12, 27570 Bremerhaven, Germany*
[b] *University of Liège, Chemical Oceanography Unit, Allée du 6 Août, 17, 4000 Liège, Belgium*
[c] *Leibniz Institute of Marine Sciences, IfM-GEOMAR, Biological Oceanography, Düsternbrooker Weg 20, 24105 Kiel, Germany*

ARTICLE INFO

Article history:
Received 21 April 2011
Received in revised form 3 October 2011
Accepted 4 October 2011
Available online 1 November 2011

Keywords:
Carbonate system
Chemostat
CO_2
Emiliania huxleyi
Stoichiometry
Temperature

ABSTRACT

The present study investigates the combined effect of phosphorous limitation, elevated partial pressure of CO_2 (pCO_2) and temperature on a calcifying strain of *Emiliania huxleyi* (PML B92/11) by means of a fully controlled continuous culture facility. Two levels of phosphorous limitation were consecutively applied by renewal of culture media (N:P = 26) at dilution rates (D) of 0.3 d^{-1} and 0.1 d^{-1}. CO_2 and temperature conditions were 300, 550 and 900 µatm pCO_2 at 14 °C and 900 µatm pCO_2 at 18 °C. In general, the steady state cell density and particulate organic carbon (POC) production increased with pCO_2, yielding significantly higher concentrations in cultures grown at 900 µatm pCO_2 compared to 300 and 550 µatm pCO_2. At 900 µatm pCO_2, elevation of temperature as expected for a greenhouse ocean, further increased cell densities and POC concentrations. In contrast to POC concentration, C-quotas (pmol C $cell^{-1}$) were similar at $D = 0.3\ d^{-1}$ in all cultures. At $D = 0.1\ d^{-1}$, a reduction of C-quotas by up to 15% was observed in the 900 µatm pCO_2 at 18 °C culture. As a result of growth rate reduction, POC:PON:POP ratios deviated strongly from the Redfield ratio, primarily due to an increase in POC. Ratios of particulate inorganic and organic carbon (PIC:POC) ranged from 0.14 to 0.18 at $D = 0.3\ d^{-1}$, and from 0.11 to 0.17 at $D = 0.1\ d^{-1}$, with variations primarily induced by the changes in POC. At $D = 0.1\ d^{-1}$, cell volume was reduced by up to 22% in cultures grown at 900 µatm pCO_2. Our results indicate that changes in pCO_2, temperature and phosphorus supply affect cell density, POC concentration and size of *E. huxleyi* (PML B92/11) to varying degrees, and will likely impact bloom development as well as biogeochemical cycling in a greenhouse ocean.

1. Introduction

During the anthropocene, atmospheric CO_2 increased from a concentration of ~280 µatm at the beginning, to 380 µatm in the year 2008, and is predicted to rise further up to 750 µatm (Houghton et al., 2001) or even >1000 µatm by the end of this century (Meehl et al., 2007; Raupach et al., 2007; Raven et al., 2005). Dissolution of CO_2 in the ocean will lead to a lowering of pH in surface waters on the order of 0.5 units over the next 100 years (Caldeira and Wickett, 2003). This acidification of the ocean is projected to be accompanied by an increase in sea surface temperature (SST) ranging between 1.1 and 6.4 °C as a consequence of climate change (Meehl et al., 2007). The increase in temperature will induce complex environmental changes such as surface seawater freshening due to sea-ice-melt, stronger water-column stratification and rising irradiance levels in surface waters (Boyd and Doney, 2002; Sarmiento et al., 2004). Responses of individual plankton species or natural communities to rising pCO_2 and temperature have been investigated in several perturbation experiments accomplished with a variety of experimental approaches concerning CO_2 manipulation, e.g. addition of HCl/NaOH (Riebesell et al., 2000), or aeration with gas of a defined CO_2 concentration (Sciandra et al., 2003), and the type of cultivation, e.g. batch cultures (Iglesias-Rodriguez et al., 2008), mesocosms (Delille et al., 2005; Engel et al., 2005; Riebesell et al., 2007), semi-continuous/dilute batch cultures (Feng et al., 2008; Riebesell et al., 2000) or chemostats (Leonardos and Geider, 2005; Sciandra et al., 2003). These studies indicate that physiological processes such as growth (Feng et al., 2008), primary production (Egge et al., 2009), calcification (Delille et al., 2005), the efficiency and regulation of carbon concentration mechanisms (CCM) (Rost et al., 2003) and the production of extracellular organic matter (Engel, 2002) are affected by changes in pCO_2.

Coccolithophores play a major role in the global carbon cycle and are known to be sensitive to rising pCO_2 (Paasche, 2002; Thierstein and Young, 2004). The expected changes in the ocean carbonate chemistry will thus likely affect the performance of coccolithophores, and may change global biogeochemical cycling in the future (Gattuso and Buddemeier, 2000). *Emiliania huxleyi*, a prominent cosmopolitan species of coccolithophores, was investigated in field, batch and

* Corresponding author. Tel.: +49 431 600 1510; fax: +49 431 600 4446.
E-mail address: aengel@ifm-geomar.de (A. Engel).

0022-0981/$ – see front matter © 2011 Elsevier B.V. All rights reserved.
doi:10.1016/j.jembe.2011.10.004

chemostat studies under a variety of growth rates and nutrient concentrations. *E. huxleyi* has a low affinity for CO_2 and a low efficient CCM and is therefore suggested to be carbon limited in the present day ocean (Paasche, 2002; Rost et al., 2003). Under nutrient replete conditions, *E. huxleyi* generally increases photosynthetic rates and concentrations of produced particulate organic carbon (POC) while grown at high pCO_2 (Riebesell et al., 2000; Rost et al., 2003; Zondervan et al., 2001). At nitrogen limitation however, elevated pCO_2 (700 µatm) led to decreased photosynthetic rates and C cell quotas (Sciandra et al., 2003), while a non-calcifying strain of *E. huxleyi* grown at phosphorous limitation was found to exhibit higher cellular POC at high pCO_2 concentrations of 2000 µatm (Leonardos and Geider, 2005). Continuous culture experiments with *E. huxleyi* revealed that sole nutrient limitation generally increases cell quotas for POC, especially under phosphorous control (Paasche, 1998; Riegman et al., 2000). With respect to calcification in coccolithophores, increasing pCO_2 was found to either decrease (Berry et al., 2002; Riebesell et al., 2000; Rost et al., 2003; Sciandra et al., 2003; Zondervan et al., 2002) or increase the concentration of biogenic calcite produced (Iglesias-Rodriguez et al., 2008) or induce complex responses (Langer et al., 2006; Langer et al., 2009).

In order to better estimate effects of global change on *E. huxleyi*, and potential consequences for biogeochemical cycling in the ocean, a better understanding of individual and combined effects of pCO_2, temperature and growth conditions, and other environmental factors, such as nutrients and light, is required (Engel, 2010; Riebesell et al., 2010; Rost et al., 2008). Therefore, we used a chemostat set-up to address combined pCO_2 and temperature effects on *E. huxleyi* under two controlled levels of phosphorous depletion. We further give a detailed description of the CO_2–aeration system used in this study and advocate that pCO_2- and temperature-controlled continuous culture facilities are likely to be an important tool for future ocean research. Earlier studies with *E. huxleyi* (PML B92/11) revealed increased POC production at elevated CO_2 (Riebesell et al., 2000) and temperature (Langer et al., 2007) while grown at nutrient replete conditions. In the future, the rise in CO_2 and temperature will occur simultaneously and is likely to be accompanied by changed nutrient conditions. Therefore, we tested for the combined effect of elevated CO_2 and temperature on inter alia POC production under phosphorous limiting conditions in order to investigate a more realistic greenhouse ocean scenario.

2. Methods

2.1. The chemostat

Chemostats allow for the full control of growing conditions during the cultivation of plankton organisms and were originally developed for the investigation of bacterial physiology by Monod (1950) and Novick and Szilard (1950). In chemostats, the cell yield is controlled by the concentration of nutrients, while the growth rate μ (d^{-1}) is balanced to the dilution rate D (d^{-1}), which is defined as

$$D = \frac{F}{V} \quad (1)$$

with F (mL d^{-1}) for the rate of inflow of nutrient media, and V (mL) for total volume of the incubator. The steady state for cell growth is reached when cell densities remain constant over time, as the dilution rate (D) equals the growth rate (μ).

$$\frac{dx}{dt} = 0,\ \mu x - Dx = 0 \text{ and therefore } \mu = D \quad (2)$$

Thus, the continuous culture method provides balanced growth of unicellular microorganisms under a defined and constant resource supply. This is true for all D lower than the maximum growth rate (μ_{max}). If $D > \mu_{max}$, the flow through exceeds cell growth and cells are washed out from the chemostat.

The set-up of one chemostat and its associated components used in this study, i.e. the incubator, thermostat, medium reservoir, peristaltic pump and overflow bottle is shown in Figs. 1 and 2. The incubator, in which the cells are grown, is a double jacketed cylindrical Plexiglas® container (60 cm height * 15 cm diameter) with a culture volume of 9.2 L. The temperature inside the incubator is regulated by a thermostat (Lauda, Ecoline Staredition, RE 104, maximum water turnover rate of 17 L min^{-1}, temperature range of −10 to +150 °C) connected to the water jacket with an approximate volume of 7 L by silicon tubes. The incubator is continuously supplied with sterile-filtered (Sartobran P 0.2 µm capsule, Sartorius) nutrient media through an inlet in the base of the incubator by peristaltic pumping (Ismatec, Ecoline) from a 100 L reservoir using silicon tubes. Excess culture medium, including suspended organic and inorganic matter, is removed through an overflow near the top of the cylinder via silicon tubes and collected in 10 L bottles. The liquid path is interrupted, as the excess medium from the incubator drips into the overflow bottle to prevent bacterial contamination from the overflow bottle into the incubator. Aeration, out-gassing, sampling and monitoring of pH and temperature inside the incubator by probes are accomplished through openings in the closure head. Excess gas leaving the incubator is channelled through a sterile 0.2 µm filter (Midisart 2000, Sartorius) to prevent contamination of the culture media from air.

Inside the incubator, a vertical stirrer with 5 horizontal stainless steel rotators is fixed to the middle of the lid. The stirrer covers the total length of the incubator and is driven by an external motor with a speed regulator (range: 20–100 rotations min^{-1}). Light supply (total irradiance and spectral composition) and the light/dark cycle

Fig. 1. Components of one chemostat connected to the CO_2 regulation system. Incubator (①), thermostat (②), peristaltic pump (④), 100 L nutrient medium reservoir (③) and overflow bottle (⑤).

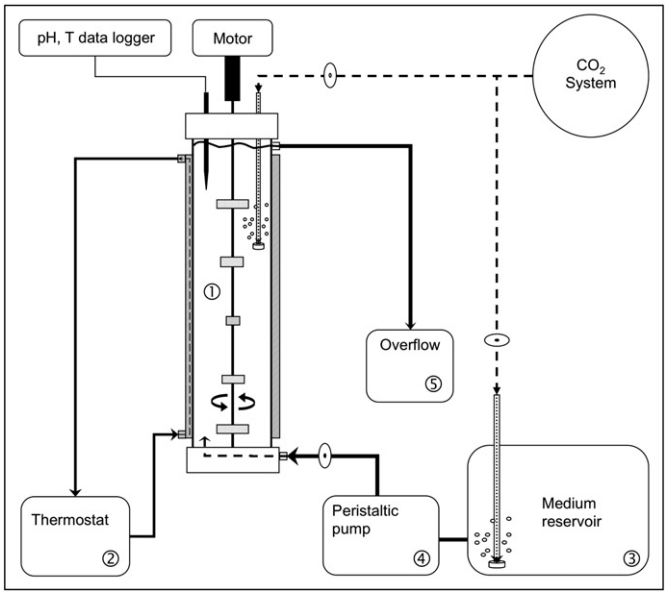

Fig. 2. The incubator and associated components. The incubator, (①) in which the cells are grown is surrounded by a water jacket that is connected to a thermostat (②) in order to control the temperature. From a separate 100 L nutrient medium reservoir (③), the incubator is continuously supplied with pre-filtered nutrient media by peristaltic pumping (④). Spent media and suspended material is removed from the incubator through an outflow and collected in an overflow bottle (⑤). The culture media in the incubator and its associated reservoir are continuously aerated with gas of preset CO_2 values using a CO_2 regulation system. Cells are kept in suspension by mechanical stirring. pH and temperature are measured and logged hourly.

can be adjusted individually for each chemostat (TL-D Delux Pro, Philips; QSL 100, Biospherical Instruments, Inc.).

Before usage, all pipes and tubes connected to the incubator were rinsed first with 10% hydrochloric acid (HCl), subsequently with deionised water, and then sterilised by autoclaving at 121 °C for 30 min. All non-autoclavable parts, like the incubator and the reservoir vessels, are cleaned with phosphate-free detergent, then soaked in 10% HCl for 2 h and thoroughly rinsed with deionised water thereafter.

2.2. The CO_2 regulation

CO_2 concentrations of the culture media in the incubator and the associated reservoir are adjusted by constant aeration with prescribed air/CO_2-mixtures in the range from 0 to 5000 µatm ±1.8% using a CO_2 regulation system (Figs. 1 and 3). A CO_2 scrubber is used to produce CO_2-free air from ambient air to <1 ppm CO_2 (CO2RP280, domnick hunter). The target CO_2 concentration is reached by mixing pure CO_2 (CO_2 grade 4.5; ≥99,995 Vol.%; Air Liquide, Germany) with CO_2-free air in two dilution steps, using commercially available mass flow controllers (MFC, Type 1179 Mass Flo Controller; MKS Instruments, Germany). The gas flow (F), given as standard cubic centimetre min^{-1} (sccm), through each MFC can be set separately using a digital control panel (Type 647C Multi Gas Controller; MKS Instruments Germany; accuracy 0.7%).

For the pre-dilution, a precise flow (F_a) of pure CO_2 (999.950 µatm; 99.995 Vol.%) is combined with a precise flow of CO_2-free air (F_b) (0 µatm, 0%) and channelled into a pressure vessel, in which the two gases are thoroughly homogenised. CO_2 concentrations in the gas mixture after the pre-dilution (CO_{2pre}) can be calculated from:

$$CO_{2pre(\mu atm)} = \frac{F_{a(sccm)}}{F_{b(sccm)}} \times CO_{2pure(\mu atm)}. \quad (3)$$

The pressure vessel provides a pressure difference of 0.7–2.75 bar to the subsequent MFC, which is a technical requirement for a stable gas flow towards the subsequent MFC. In order to remove excess gas above 2.75 bar, the pressure vessel is equipped with an overpressure valve, connected to the outside air via gas-tight tubes.

For the dilution to target values, the flow (F_c) of this pre-mixed gas (CO_{2pre}) is down-regulated to the target CO_2 concentration (CO_{2tar}) by another dilution with CO_2-free air (F_d) and can be calculated as follows:

$$CO_{2tar(\mu atm)} = \frac{F_{c(sccm)}}{F_{d(sccm)}} \times CO_{2pre(\mu atm)}. \quad (4)$$

Each chemostat is individually connected to the CO_2 regulation system. For the setup of five chemostats a total of twelve MFC is needed; two MFC to create a homogenous CO_2/air mixture in the pressure vessel and another two MFC for each chemostat to conduct the mixing step to target values. In order to remove dust and bacteria, the gas with the target CO_2 concentration is sterile-filtered (Midisart 2000; 0.2 µm, Sartorius) and piped through silicon tubes into each chemostat and its associated reservoir (Fig. 2). The gas should be humidified by channelling through a washing flask filled with sterilised CO_2-free seawater, while using smaller volumes of culture media (<5 L). Fine bubbling of the CO_2-airstream within the incubators is mediated by gas distribution tubes (ROBU; Type A, Por. 1). All pipes of the CO_2 system are connected leak tight by ¼″ Swagelok® fittings.

2.3. Technical evaluation of the system

Precision and stability of the CO_2 regulation system was tested over a period of 7 d by applying 200, 370 and 760 µatm CO_2 by measuring the actual CO_2 concentration in the air-streams with an infrared CO_2 analyser (LI-COR, 6252). In order to test pCO_2 and temperature control in cell-free seawater, four chemostat incubators were filled with artificial seawater (salinity of 32; Tropic Marin® Sea Salt, Dr. Biener GmbH, Germany) and aerated with target CO_2 concentrations of 200, 370 and 760 µatm at 3 °C and 760 µatm at 5 °C over a period of 6 d. CO_2 concentrations in seawater were calculated from total

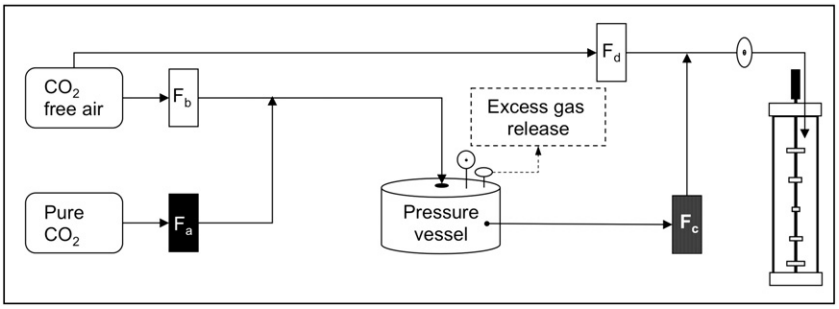

Fig.3. Simplified scheme of the CO_2 regulation system. Pure CO_2 (F_a) is combined with CO_2-free air (F_b) and channelled into a pressure vessel for thoroughly mixing. This pre-mixed gas (F_c) is down-regulated to the target CO_2 value by another dilution with CO_2 free air (F_d). Excess CO_2 gas from the pressure vessel is discharged to an exhaust system.

alkalinity (TA, 2440 μmol kg^{-1} seawater (SW)) and pH (see measurements and analysis). Once the pre-test yielded precise and stable performance of the CO_2–aeration system, it was applied to five chemostats for the main experiment with *E. huxleyi*.

2.4. Experiment with E. huxleyi

A calcifying strain of *E. huxleyi* (PML B92/11) was grown in five chemostats. pCO_2 and temperature were set to 300 μatm at 14 °C, 550 μatm at 14 °C and 18 °C, and 900 μatm at 14 °C and 18 °C (hereafter referred to as 300-14, 550-14, 550-18, 900-14 and 900-18). Before the experiment, cells were grown in 10 L Nalgene bottles as separate inoculum culture in modified f/2-medium (Guillard and Ryther, 1962): Natural seawater was enriched to 100 μmol L^{-1} NO_3^-, 10 μmol L^{-1} PO_4^{3-} and full metal mix and vitamins were added. Culture medium for the chemostat experiment was prepared from natural seawater with a salinity of 32, pH of 7.97 and TA of 2281 μmol kg^{-1} SW and enriched with macronutrients to yield final concentrations of 29 μmol L^{-1} NO_3^- and 1.1 μmol L^{-1} PO_4^{3-} to favour phosphorous limiting conditions. After the addition of a metal mix, according to the f/2-medium (Guillard and Ryther, 1962), the medium was pre-filtered (Sartobran P, 0.2 μm capsule, Sartorius) and treated with UV irradiation (Microfloat 1/0, a.c.k. aqua concept GmbH) for 3 h for sterilisation. Thereafter, f/2 vitamins were added thereafter in order to prevent photo-degradation. A total of 9.2 L medium was filled into each chemostat incubator. Temperature control and aeration were adjusted and allowed to equilibrate for 2 d. Then, the cells were inoculated to each of the five chemostats to a final density of 3000 cells mL^{-1}, and grown in batch mode, i.e. without flow-through, for 3 d. Thereafter, the continuous flow was started for all chemostats and kept for 12 d at $D=0.3\ d^{-1}$, followed by another 12 d at $D=0.1\ d^{-1}$. The chemostats were run as cyclostats with a light:dark cycle of 16 h:8 h in order to simulate a natural day:night cycle with an irradiance of 300 μmol photons $m^{-2}\ s^{-1}$. Gentle mixing of the culture at 50 rotations min^{-1} was applied during this study to keep cells in suspension.

Three samplings for each dilution rate were accomplished on days 10, 14 and 17 for $D=0.3\ d^{-1}$ and days 22, 25 and 28 for $D=0.1\ d^{-1}$ of the experiment. Sample volume did not exceed 10–15% of the culture volume to avoid significant perturbations of the steady state (Hutchins et al., 2003). Daily cell counts and samplings of all other parameters were conducted at the same time of the day (3 h after lights on) in order to avoid biases resulting from diel rhythms.

2.5. Cell density and chemical analysis

Cell density and biovolume were determined daily as the mean of three consecutive measurements of 500 μl by an electronic particle counter (Coulter Multisizer III, Beckman Coulter) equipped with a 100 μm aperture. Samples were diluted 1:100 with 0.2 μm pre-filtered (Minisart 2000, Sartorius) seawater with a salinity of 32. Particles with an equivalent spherical diameter in a range of 3.27 μm to 7.96 μm were identified as *E. huxleyi*, after microscopic inspection. For a continuous culture, variations in cell density of <10% for three consecutive days has been suggested as a practical criteria for physiological steady state (Leonardos and Geider, 2005).

For total particulate carbon (TPC), particulate organic carbon (POC), particulate organic nitrogen (PON) and particulate organic phosphorous (POP), 100 mL sample were filtered onto pre-combusted (8 h at 500 °C) glass fibre filters (GF/F, Whatman) in duplicates. POC filters were acidified by adding 3–5 drops of 0.2 M HCl on top of the filter to remove particulate inorganic carbon (PIC) and dried overnight at 60 °C. Total and organic particulate C- and N-concentrations were determined with an elemental analyzer (EuroEA, Euro Vector). PIC was calculated as the difference between TPC and POC. For dissolved organic phosphorous (DOP), 35 mL GF/F filtrate were stored frozen at −20 °C until analysis. POP and DOP were determined colorimetrically after persulfate oxidation with a precision of ±0.02 μmol L^{-1} (Koroleff and Grasshof, 1983).

For determination of TA, 200 mL of sample was filtered through pre-combusted (8 h, 500 °C) glass fibre filters (Whatman, GF/F). The filtrate was stored in 200 mL PE bottles at 0 °C in the dark. Measurements were carried out by the titration method with 0.1 M HCl (Gran, 1952), with a precision of ±3 μmol kg^{-1} SW. Data were quality checked by the analysis of Certified Reference Material required from Andrew Dickson (Scripps Institution of Oceanography, University of California, San Diego) with an accuracy of <3 μmol kg^{-1} SW. pH and temperature within the incubators were measured with a proton sensitive combined pH–temperature electrode (Sentix 41; WTW standard DIN/NBS buffers PL 4, PL 7 and PL 9) and recorded hourly on a data logger (WTW; pH 340i) throughout the experiment. Accuracy of pH measurement was better than ±0.01 pH units and ±0.1 °C for temperature. pCO_2, total dissolved inorganic carbon (DIC), carbonate (CO_3^{2-}), bicarbonate (HCO_3^-) and Ω calcite in chemostat cultures and medium reservoirs were calculated from $pH_{(NBS)}$ and TA values of each sampling time using the program CO2sys (Lewis and Wallace, 1998), with the carbonic acid dissociation constants of Mehrbach et al. (1973) refitted by Dickson and Millero (1987), the HSO_4^- dissociation constant of Dickson et al. (1990) on the U.S. National Bureau of Standards scale. The saturation state (Ω) of calcite was computed using the calcite solubility of Mucci (1983). Phosphate concentrations of the initial reservoir medium were implemented in the calculation. Nitrate was added as $NaNO_3$, which has no effect on TA (Gattuso et al., 2010).

For nutrients, 50 mL sample were filtered through 0.2 μm (Minisart 2000, Sartorius) syringe filters and frozen at −20 °C until analysis. Measurements of NO_3^- and PO_4^{3-} were made spectrophotometrically after Grasshoff et al. (1999) (Autoanalyzer Evolution 3, Alliance Instruments). Detection limits were 0.3 μmol L^{-1} for N and 0.1 μmol L^{-1} for P.

2.6. Data treatment

For statistical analysis, data of each sampling for both growth rates were implemented in calculations. Differences were tested by means of analysis of co-variance (two-way ANOVA) with factors being the dilution rate (D) and the CO_2/temperature-treatment, respectively. Furthermore, differences in cell densities, cell size and biovolume between CO_2/temperature-treatments were tested by means of a t-test. Statistical significance was accepted for $p<0.05$. All calculations were performed using the software package Sigma Plot 10.01 (SysStat).

3. Results

3.1. Evaluation of temperature control and CO_2 regulation

The pre-tests showed good stability of CO_2 concentrations in gas streams obtained by the CO_2 regulation system. Concentrations of 200, 370 and 760 μatm CO_2 in airstreams were stable over a period of 7 d within standard deviations of ±0.7, ±1.7 and ±1.6%, respectively. Equilibration of gas with preset CO_2 concentrations in artificial seawater was reached after a maximum of 60 h, observed by the development of pH (Fig. 4, Table 1). As temperature control was set before slowly filling the incubator with seawater, target temperatures of 3 and 5 °C were reached immediately and remained stable with a maximum standard deviation of ±0.1 °C (Table 1).

3.2. Experiment with E. huxleyi

3.2.1. Growth and cell densities

During the initial batch phase, growth of *E. huxleyi* was significantly accelerated by increased temperature, as cells grew at mean

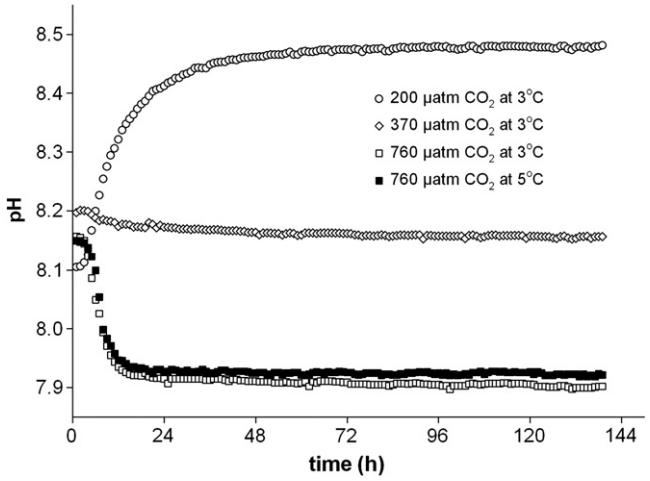

Fig. 4. Equilibration of CO_2 in artificial seawater. Concentrations of 200, 370 and 760 µatm CO_2 were set in the air-streams and equilibration at 3 and 5 °C was followed by the development of pH. Target values were reached after maximum 60 h.

growth rates of $1.21 \pm 0.09\ d^{-1}$ in 18 °C cultures compared to $0.83 \pm 0.00\ d^{-1}$ in 14 °C cultures (*t*-test, $p = 0{,}016$). A strong build up of biomass occurred in all cultures during the transition from nutrient replete to deplete conditions, until steady state for growth at $D = 0.3\ d^{-1}$ was reached between days 10 and 12 of the experiment (Fig. 5). Sampling 1 (day 10) was omitted for data evaluation because the growth rate did not equal the dilution rate in the 300-14, 550-14 and 900-14 cultures at that time, indicating, that growth was not at steady state. Cell density of the 550-18 culture declined from day 14 onwards and was not included in this study further.

Induced by CO_2 and temperature, different steady state cell densities were determined among cultures while grown on identical nutrient concentrations. Relative to the 300-14 culture, cell densities in 900-14 and 900-18 cultures were significantly increased by 16 and 36% (*t*-test, $n = 17$; $p < 0.001$), respectively, while the difference between 300-14 and 550-14 cultures was not significant (Figs. 5 and 6, upper panel). The dilution rate was reduced on day 17 from $D = 0.3\ d^{-1}$ to $D = 0.1\ d^{-1}$ and growth rates of all cultures adapted to the changed medium supply within 2 days, while cell densities remained constant throughout the experiment with deviations <10.6% (Table 2).

3.2.2. Cell volume and total biovolume

At $D = 0.3\ d^{-1}$, cell volume was similar in all cultures varying in a range of 69–75 $\mu m^3\ cell^{-1}$ (Table 2). While grown at $D = 0.1\ d^{-1}$, volume of 900-14 and 900-18 cells was significantly reduced by 12 and 24%, respectively, in relation to cells of the same cultures grown at $D = 0.3\ d^{-1}$ (*t*-test, $n = 6$ vs. 9, $p = 0.032$ and $p < 0.001$). Since cell volume at $D = 0.1\ d^{-1}$ only decreased in 900-14 and 900-18 cultures, these cells were 11 and 25% smaller relative to the volume of 300-14 and 550-14 cells (*t*-test, $n = 9$, $p = 0.034$ and $p < 0.001$) (Table 2). These observations are reflected in the total biovolume, derived from cell density and single cell volume (Fig. 5). While grown at $D = 0.3\ d^{-1}$, the total biovolume was elevated by 21 and 30% in 900-14 and 900-18 cultures relative to the 300-14 culture due to higher cell densities of cells with comparable volume (*t*-test, $n = 6$ vs. 9; $p < 0.05$). At $D = 0.1\ d^{-1}$, total biovolume was similar in all cultures as a consequence of the reduced volume of 900-14 and 900-18 cells (Fig. 5).

Table 1
Target and actual post-equilibration temperature, pCO_2 and pH for the test in artificial seawater ($n = 84$) and for the *Emiliania huxleyi* experiment ($n = 24$). Target pH values were calculated from target pCO_2 together with the initial TA of nutrient media (2440 and 2281 µmol kg^{-1} SW for artificial and natural SW, respectively). Mean values are given ± standard deviations in parentheses.

	Target			Post-equilibration		
	T (°C)	pCO_2 (µatm)	pH	T (°C)	pCO_2 (µatm)	pH
Artificial seawater	3.0	200	8.43	3.0 (0.0)	173 (5)	8.48 (0.01)
	3.0	370	8.20	3.0 (0.1)	383 (10)	8.18 (0.01)
	3.0	760	7.91	2.9 (0.0)	768 (26)	7.91 (0.02)
	5.0	760	7.91	4.9 (0.1)	735 (43)	7.92 (0.02)
E. huxleyi experiment	14.0	300	8.28	14.2 (0.1)	287 (6)	8.29 (0.01)
	14.0	550	8.05	14.2 (0.1)	543 (4)	8.05 (0.00)
	14.0	900	7.85	14.2 (0.1)	897 (17)	7.86 (0.01)
	18.0	900	7.87	18.1 (0.1)	882 (14)	7.86 (0.01)

3.3. Nutrient assimilation and C:N:P stoichiometry

The mean molar ratio of PON:POP of 25.5 ± 3.0 in all cultures throughout both growth rates mirrored the molar DIN:DIP ratio of 26 in supplied nutrient media. Residual DIN concentrations in a range of 0.42–1.08 µmol L^{-1} were determined in culture media of all cultures, while DIP was always below the detection limit, indicating an exclusive phosphorous depletion. Changes in CO_2 and temperature induced different cell densities on identical nutrient supply. Therefore, cellular POP and PON production and cell quotas for POP and PON (P- and N-quotas) exhibited a decreasing trend with increasing CO_2 and temperature (Fig. 6, lower panel and Table 2). Within each culture, PON production and therefore N-quotas remained unaffected by the changed growth rate (Table 2). This observation also holds for POP except for the 900-18 culture for which a clearly lower POP production and P-quota at $D = 0.1\ d^{-1}$ were determined (Table 2). At $D = 0.3\ d^{-1}$, the molar PON:POP ratio was lowest with a value of 21 for 900-18 cells. In contrast, while grown at $D = 0.1\ d^{-1}$, molar PON:POP ratio was highest in the 900-18 culture with 28, due to the lowered POP.

Dissolved organic nitrogen (DON) was not determined during this study but could be estimated from the difference between the sum of DIN and PON in chemostats and DIN in the medium reservoir. In the 300-14 culture, DON:PON varied between 0.39 and 0.45 and ratios were more than doubled compared to averaged 0.19 ± 0.09 in the other cultures. DOP concentrations were generally below the detection limit.

During this study, clear differences in POC dynamics were determined among cultures as a response to growth rates, CO_2 and temperature on total and cell normalised levels. Relative to rates at $D = 0.3\ d^{-1}$, POC production was significantly reduced in all cultures at $D = 0.1\ d^{-1}$ (two-way ANOVA, $p < 0.001$). At $D = 0.3\ d^{-1}$, POC production (µmol $L^{-1}\ d^{-1}$) was significantly higher in the 900-18 culture (two-way ANOVA, $p < 0.001$) compared to all other cultures, and generally increased with rising CO_2 and higher temperature (Fig. 6, middle panel). In contrast to total production of POC (µmol $L^{-1}\ d^{-1}$), cell normalised POC production (pmol $cell^{-1}\ d^{-1}$) was not affected by CO_2 and temperature at $D = 0.3\ d^{-1}$ (Fig. 6, lower panel). No statistical significant difference in POC production (µmol $L^{-1}\ d^{-1}$) among cultures was determined for $D = 0.1\ d^{-1}$ and cell normalised POC production (pmol $cell^{-1}\ d^{-1}$) and carbon cell quotas (C-quotas, pmol $cell^{-1}$) for POC even exhibited an inverted trend at $D = 0.1\ d^{-1}$ with lowest values in the 900-18 culture (Table 2).

POC production was decoupled from cell growth which led to significantly higher POC concentrations and C-quotas at $D = 0.1\ d^{-1}$ (two-way ANOVA, $p < 0.001$ and $p < 0.001$) (Table 2). The relative increase of POC concentration was greatest in the 300-14 culture, resulting in 39% more POC and highest C-quota after the change from $D = 0.3\ d^{-1}$ to $D = 0.1\ d^{-1}$. While C-quotas at $D = 0.1\ d^{-1}$ decreased with increasing CO_2 and temperature (Table 2), POC concentration (µmol L^{-1}) was significantly higher in the 900-18 culture

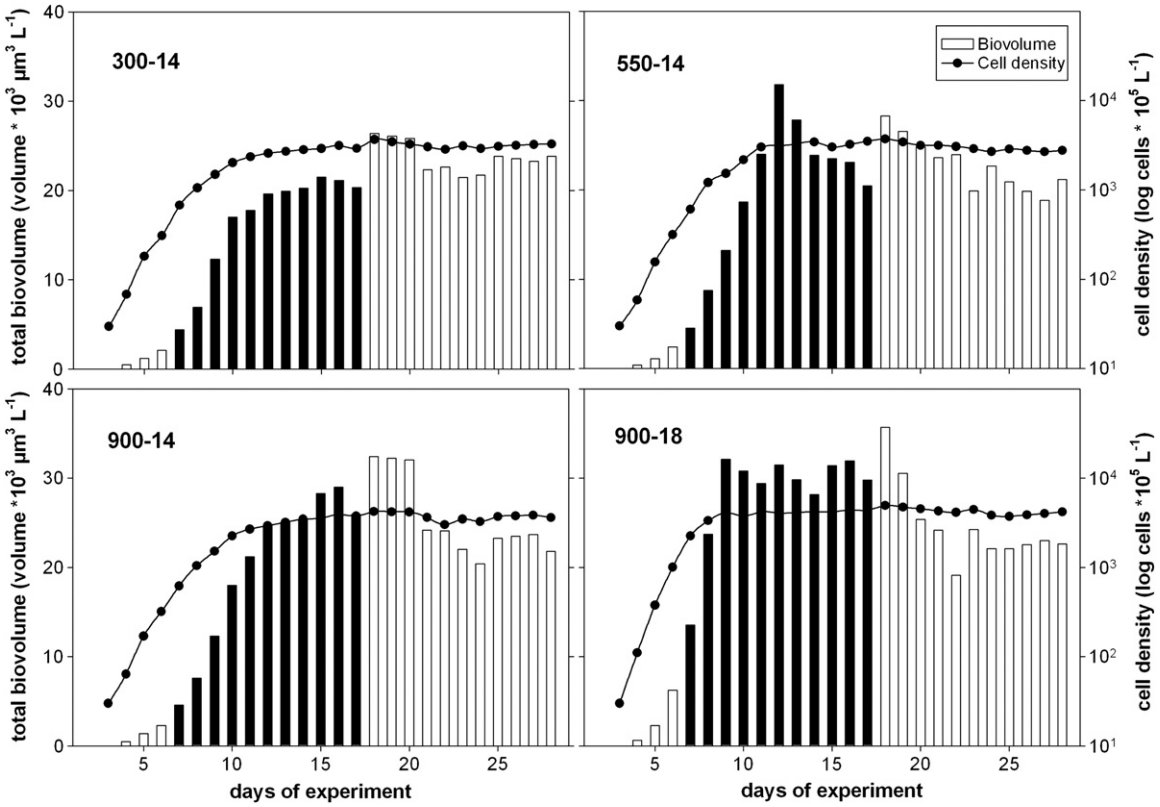

Fig. 5. *Emiliania huxleyi* cell densities (circles) and total biovolume (bars) during the course of the experiment. Cells were inoculated on day 3 of the experiment and grown in batch mode until a dilution rate (D) of $D=0.3\ d^{-1}$ was applied on day 5 and reduced to $D=0.1\ d^{-1}$ on day 17. The samplings were accomplished on days 10, 14 and 17 for $D=0.3\ d^{-1}$ and on days 22, 25 and 28 for $D=0.1\ d^{-1}$. On day 10 the steady state was reached only in the culture grown at 900 µatm CO_2 and 18 °C. From day 12 onwards cell densities remained constant in all cultures within maximum deviations of 10.6%.

throughout both growth rates (*t*-test, $n=5$; $p<0.05$), likely due to the higher cell density in cultures grown at elevated CO_2 and temperature.

Changes in POC were accompanied by large deviations of the elemental composition of biomass from the Redfield ratio. During this study, ratios were most affected by changes in growth rate, and to a lesser degree by CO_2 and temperature. Molar POC:PON at $D=0.3\ d^{-1}$ ranged from 25.6 ± 2.0 in the 300-14 culture to maximum ratios of 29.5 ± 0.2 in the 900-18 culture, respectively. At $D=0.1\ d^{-1}$, due to the strongest relative increase of POC in the 300-14 culture, the molar POC:PON of this culture was elevated to a greater extend than in all other cultures and now equalled the ratio of the 900-18 culture with 41 ± 1. Molar POC:POP ratios varied from 642 ± 47 to 732 ± 143 at $D=0.3\ d^{-1}$ and yielded a maximum of 1142 ± 9 in the 900-18 culture due to high POC relative to very low POP at $D=0.1\ d^{-1}$.

3.4. Carbonate system and particulate inorganic carbon (PIC)

Averaged pCO_2 values including the two growth rates were $261\pm12\%$ (300-14), $536\pm3\%$ (550-14), $1003\pm9\%$ (900-14) and $957\pm8\%$µatm (900-18) (Table 3). Alleged variations from target values are likely to be reasoned by the computation of pCO_2 (see Discussions section 'Impact of calcification on the carbonate system').

In addition to the uptake of DIC (CO_2) for the build up of organic compounds, calcite production led to pronounced changes of the carbonate system in all cultures. From initial values determined after equilibration (Table 1), pH dropped between 0.08 and 0.23 units after reaching the steady state for $D=0.3\ d^{-1}$. From 2281 µmol kg^{-1} SW, TA decreased by maximum 929 µmol kg^{-1} SW, in the 900-18 culture during the initial build up of biomass. Reducing the dilution rate from $D=0.3\ d^{-1}$ to $D=0.1\ d^{-1}$ again led to pronounced changes as pH dropped by up to 0.18 units and TA by up to 400 µmol kg^{-1} SW, respectively. Still, within one applied dilution rate, the carbonate system remained rather constant, as changes did not exceed 0.04 and 0.01 pH units, and 18 and 28 µmol kg^{-1} SW for TA during $D=0.3\ d^{-1}$ and $D=0.1\ d^{-1}$, respectively (Table 3).

Seawater became under-saturated with respect to calcite (Ω calcite <1) in all cultures except for the 300-14, and 550-14 culture at $D=0.3\ d^{-1}$ (Table 3). Therefore, PIC data obtained in this study have to be interpreted with caution due to possible carbonate dissolution. A detectible but not significant decrease of cell normalised PIC was observed with increasing CO_2 and temperature at both growth rates (Table 2). Total concentrations of PIC showed no significant response to either growth conditions or CO_2 or temperature. Averaging for all cultures, 101.9 ± 5.7 µmol L^{-1} and 116.6 ± 19.0 µmol L^{-1} PIC were determined at $D=0.3\ d^{-1}$ and $D=0.1\ d^{-1}$, respectively. In all cultures, high POC relative to overall low PIC, resulted in low molar PIC:POC ratios ranging from 0.14 to 0.18 at $D=0.3\ d^{-1}$ and 0.11 to 0.17 at $D=0.1\ d^{-1}$.

4. Discussion

4.1. CO_2- and temperature-control in chemostats

A simultaneous pCO_2 and temperature control to chemostats allows for the investigation of co-effects, i.e. with nutrient availability over a prolonged period of time. In comparison to other cultivation methods, the continuous culture is the only approach that enables the full control of growth at any given rate within minimum and maximum growth rate of investigated organisms. Therefore, chemostats have the great advantage to investigate distinct responses induced by environmental factors, such as CO_2 and temperature, while growth and nutrient availability are fully controlled. In the framework of

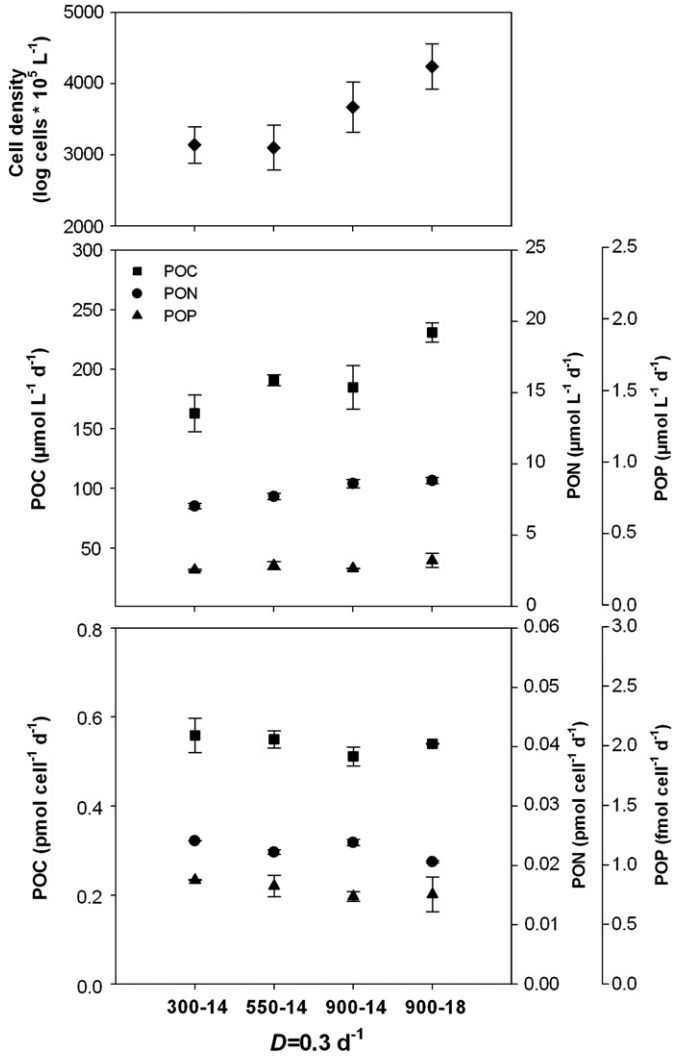

Fig. 6. *Emiliania huxleyi* cell density (upper panel, $n=16$), POC (squares), PON (circles) and POP (triangles) production on total (µmol L^{-1} d^{-1}, middle panel, $n=2$) and cell normalised (pmol and fmol $cell^{-1}$ d^{-1}, lower panel, $n=2$) levels at various CO_2 and temperature where $D=0.3$ d^{-1}.

global change, this is a valuable experimental capability, because the impacts of acidification and warming are likely to be masked by nutrient effects and growth conditions (LaRoche et al., 2010).

We chose to continuously aerate the culture media, since this method was shown to best simulate pCO_2 increase in the ocean in comparison to closed (addition of acid or base and then closing the culture vessel without headspace) and buffered (the addition of $NaHCO_3^-$, $NaCO_3^{2-}$ or organic buffers) experimental manipulations (Gattuso et al., 2010; Rost et al., 2008; Schulz et al., 2009). Testing the chemostat system without biological activity showed good stability of pCO_2 and temperature in the incubators (Table 1 and Fig. 4). Biological activity, while working with calcifying organisms, generally challenges the control of applied conditions, especially the carbonate system. A high resolution determination of the abiotic conditions and of the physiological responses of the cells is strongly suggested in order to identify potential deviations from steady state conditions. The CO_2 regulation system presented here (Fig. 3) allows for continuous adjustment of pCO_2 concentrations over a wide range.

4.2. Growth of *E. huxleyi*

During the last decades, the response of the coccolithophore *E. huxleyi* to changes in growth rates (Paasche, 1998; Riegman et al., 2000), temperature (Feng et al., 2008; Langer et al., 2007) and pH or pCO_2 has been extensively studied (Delille et al., 2005; Leonardos and Geider, 2005; Rost et al., 2003; Sciandra et al., 2003). Responses to changed seawater carbonate chemistry are suggested to vary not only among different experimental approaches, phytoplankton groups and coccolithophore-species, but even on the strain-level (Fabry, 2008; Langer et al., 2009). This study is the first to investigate combined CO_2 and temperature effects on a calcifying strain of *E. huxleyi* (PML B92/11) grown in P-controlled chemostats. Significantly higher cell densities were achieved with increasing pCO_2 and temperature during the initial replete phase and the transition to P depletion (Fig. 5). These findings are in accordance with earlier findings that suggested cell growth and POC production of *E. huxleyi* to be increased by elevated CO_2 (Riebesell et al., 2000; Rost et al., 2003) and temperature (Langer et al., 2007) under nutrient replete conditions.

Growth rates in continuous cultures are not only controlled by the dilution with fresh nutrient media, but also by the cellular nutrient

Table 2
Chemical composition of *Emiliania huxleyi* grown under various CO_2 and temperature conditions at different dilution rates (D). Values are given for growth rates (μ), cell volume, cell density, particulate organic carbon (POC), nitrogen (PON), phosphorous (POP) and inorganic carbon (PIC) cell quota. For growth rates, cell volume and cell density, mean values ± standard deviations in parenthesis are given for each steady state ($n=6$ at $D=0.3$ d^{-1} and $n=9$ at $D=0.1$ d^{-1}) and for POC, PON, POP and PIC at $D=0.3$ d^{-1} (Sampling 2 and 3) and $D=0.1$ d^{-1} (sampling 4, 5 and 6), respectively.

D [d^{-1}]	Culture	µ [d^{-1}]	Volume [μm^{-3} $cell^{-1}$]	Cell density [$*10^5$ L^{-1}]	POC [pmol $cell^{-1}$]	PON [pmol $cell^{-1}$]	POP [fmol $cell^{-1}$]	PIC [pmol $cell^{-1}$]
0.3	300 µatm CO_2 14 °C	0.32 (0.03)	70.3 (3.3)	2940 (166)	1.84 (0.13)	0.072 (0.001)	2.86 (0.01)	0.32 (0.16)
	550 µatm CO_2 14 °C	0.31 (0.03)	69.4 (6.9)	3294 (187)	1.81 (0.06)	0.069 (0.003)	2.70 (0.29)	0.30 (0.03)
	900 µatm CO_2 14 °C	0.33 (0.04)	75.0 (5.4)	3574 (274)	1.68 (0.07)	0.070 (0.002)	2.41 (0.13)	0.30 (0.07)
	900 µatm CO_2 18 °C	0.32 (0.01)	71.3 (4.0)	4243 (125)	1.77 (0.00)	0.060 (0.000)	2.47 (0.48)	0.24 (0.02)
0.1	300 µatm CO_2 14 °C	0.11 (0.02)	73.8 (3.4)	3177 (184)	2.69 (0.21)	0.066 (0.006)	3.09 (0.21)	0.44 (0.27)
	550 µatm CO_2 14 °C	0.09 (0.02)	75.2 (4.9)	2941 (247)	2.70 (0.13)	0.070 (0.007)	2.84 (0.23)	0.42 (0.01)
	900 µatm CO_2 14 °C	0.11 (0.01)	66.4 (7.2)	3663 (368)	2.52 (0.32)	0.070 (0.007)	2.50 (0.30)	0.26 (0.03)
	900 µatm CO_2 18 °C	0.09 (0.03)	55.6 (3.9)	4168 (324)	2.46 (0.12)	0.061 (0.002)	2.19 (0.08)	0.31 (0.06)

content, i.e. the cell quota (Caperon, 1968; Droop, 1968). Changes in the cell quota are therefore potentially accompanied by changes in growth rates and vice versa. During this study, cell densities in each culture, remained constant for both dilution rates. This indicates that growth rates were exclusively governed by the dilution rate, and unaffected by slight variations in cell quotas among cultures (Fig. 5 and Table 2). In the present continuous culture study cells were kept in the exponential growth phase at very low growth rates. Therefore, only a small fraction of cells was in the same growth stage and the response of the cells to the light:dark cycle became less obvious. As cell densities were constant over time, a phasing of cell division was not observed. Growth rates equalling the dilution rate thus hold on a daily basis for cell densities, as suggested for an earlier chemostat study (Fritz, 1999).

Physiological responses of *E. huxleyi* to changes in pCO_2 were investigated in previous studies with cells acclimated for more than 7 generations (Zondervan et al., 2002), after a gradual increase of pCO_2 over 152 generations (Müller et al., 2010) or in short-term response experiments (Barcelos e Ramos et al., 2010). Comparison of the results obtained by these studies indicated similar responses of acclimated and non-acclimated cells and allows the conclusion that a time scale of hours provides sufficient time for a physiological acclimation to changes in pCO_2 (Barcelos e Ramos et al., 2010). For the present study, it was therefore assumed that cells were fully acclimated to applied pCO_2 conditions before the steady state was reached after 10 and 12 days, respectively.

4.3. Impact of calcification on the carbonate system

During this study, growth of *E. huxleyi* led to significant changes in the carbonate chemistry of the culture media (Table 3). During calcification (precipitation of $CaCO_3$), DIC and TA are reduced and the shift of the chemical equilibrium of the carbonate system leads towards higher $CO_{2(aq)}$ concentrations and lower pH values (Zeebe and Wolf-Gladrow, 2001). Although our data showed that the carbonate system remained stable at a given dilution rate, the initial build up of coccolithophore biomass and thus of biogenic calcite led to strong DIC and TA draw down that exceeded the amounts of DIC and TA replenished from the reservoir. This points to a more general problem while working with calcifying organism at low dilution rates in chemostats. As observed for the high cell densities of *E. huxleyi* during this study, calcification and the consequent draw down of TA in the incubator cannot be balanced by medium supply, leading to a decrease of TA in the incubator and therefore alterations of the whole carbonate speciation. To balance the draw down of TA during the build-up of biomass in the initial batch phase of chemostat experiments, it is recommended to either adjust TA what can be done by adding $NaHCO_3$ (Gattuso et al., 2010; Rost et al., 2008), or to reduce the cell density (LaRoche et al., 2010). If an online regulation of TA is desired throughout the experiment, at least two components of the carbonate system should be monitored daily. Although high resolution measurements of pH and pCO_2 are easier to accomplish, both depend strongly on H^+ and to a lesser extend on CO_3^{2-} and HCO_3^-. For the computation of the carbonate system, the combination of pH and pCO_2 therefore might lead to large errors for TA and DIC (Millero, 1995).

Throughout this study, distinct pCO_2-levels were achieved and sustained for each of the cultures. However, calculated pCO_2-values were slightly lower than target values in 300 and 550 µatm and up to ~100 µatm higher in 900 µatm cultures (Table 3). This deviation is likely due to practical constraints. pH was measured every hour, while TA was determined for the days of sampling. Therefore, calculations of pCO_2 from pH and TA were accomplished for individual timepoints only. Also, accumulation of dissolved organic carbon (DOC) in culture experiments has been recently suggested as a possible cause for discrepancies in the internal consistency of inorganic carbon

Table 3
Carbonate system during the *Emiliania huxleyi* experiment. Mean ($\bar{X}$), minimum (min), maximum (max) values and standard deviations (SD%) are given for $D = 0.3\ d^{-1}$ (sampling 2 and 3) and $D = 0.1\ d^{-1}$ (sampling 4, 5 and 6), respectively.

Culture	Dilution rate (d^{-1})	pH		TA (µmol kg^{-1} SW)		pCO_2 (µatm)		CO_2 (µmol kg^{-1} SW)		DIC (µmol kg^{-1} SW)		HCO_3^- (µmol kg^{-1} SW)		CO_3^{2-} (µmol kg^{-1} SW)		Ω Calcite	
		0.3	0.1	0.3	0.1	0.3	0.1	0.3	0.1	0.3	0.1	0.3	0.1	0.3	0.1	0.3	0.1
300 µatm	$\bar{X}$	8.18	8.00	1440	1031	243	274	9.5	10.7	1292	945	1191	889	91.0	44.9	2.22	1.09
pCO_2	SD%	–	–	1.9	1.9	9.7	12.3	9.7	12.3	0.9	3.4	0.3	3.7	10.3	4.6	10.30	4.59
14 °C	min	8.15	8.03	1420	1020	226	261	8.9	10.3	1283	918	1193	862	84.3	46.3	2.05	1.13
	max	8.21	8.02	1459	1054	259	248	10.2	9.7	1300	981	1189	926	97.6	45.9	2.38	1.12
550 µatm	$\bar{X}$	7.88	7.75	1435	1095	522	546	20.5	21.4	1369	1057	1298	1007	50.0	28.8	1.22	0.70
pCO_2	SD%	–	–	1.1	4.6	1.7	1.3	1.7	1.3	1.1	4.1	1.1	4.0	0.6	7.4	0.60	7.43
14 °C	min	7.88	7.77	1424	1045	516	545	20.2	21.4	1358	1099	1288	966	50.2	26.5	1.22	0.64
	max	7.89	7.76	1446	1095	528	553	20.7	21.7	1380	1059	1309	1047	49.8	29.2	1.21	0.71
900 µatm	$\bar{X}$	7.68	7.54	1517	1260	924	1056	36.3	41.4	1496	1253	1425	1191	34.3	20.8	0.84	0.51
pCO_2	SD%	–	–	0.5	1.6	12.5	0.5	12.5	0.5	0.3	1.3	0.3	1.3	11.9	2.2	11.92	2.24
14 °C	min	7.64	7.54	1512	1237	842	1051	33.1	41.2	1493	1247	1422	1185	31.4	20.4	0.76	0.50
	max	7.72	7.54	1522	1269	1005	1062	39.4	41.7	1499	1272	1428	1209	37.2	21.3	0.91	0.52
900 µatm	$\bar{X}$	7.64	7.55	1309	1153	902	994	31.4	34.6	1285	1144	1223	1088	30.9	22.1	0.76	0.54
pCO_2	SD%	–	–	1.8	1.7	13.6	0.8	13.6	0.8	2.5	1.7	2.5	1.7	8.6	3.3	8.56	3.30
18 °C	min	7.61	7.54	1293	1133	815	985	28.4	34.3	1262	1127	1201	1071	29.1	21.3	0.71	0.52
	max	7.68	7.55	1325	1153	988	999	34.4	34.8	1308	1166	1245	1108	32.8	22.1	0.80	0.54

computations (Koeve et al., 2011), although we cannot address this issue since DOC was not monitored during our experiment.

The computation of the carbonate system requires two known input parameters, e.g. DIC and TA or pH and TA. pH and TA were recently suggested to provide more reliable pCO_2-values than e.g. the TA–DIC-couple (Hoppe et al., 2010). This statement was furthermore proposed to hold true for calculations based on TA and $pH_{(NBS)}$ using the NBS-scale, even though it is generally advocated to correct $pH_{(NBS)}$ values or measure pH directly on the total hydrogen ion concentration scale using Tris (2-amino-2-hydroxymethyl-1,3-propanediol)-based pH reference materials provided by e.g. A. Dickson (see Methods section above) (Dickson, 2010).

4.4. Elemental stoichiometry and carbon overconsumption

The relative increase in carbon assimilation, decoupled from nutrient assimilation that leads to deviations from Redfields C:N:P-stoichiometry of 106:16:1 is referred to as carbon overconsumption (Toggweiler, 1993). Carbon overconsumption was reported from earlier studies conducted with *E. huxleyi* under sole nutrient limitation, or in combination with rising CO_2 (Banse, 1994; Engel et al., 2005; Leonardos and Geider, 2005; Riegman et al., 2000; Sciandra et al., 2003). During this study, different extents of P depletion combined with elevated CO_2 and temperature induced massive changes in elemental stoichiometry of organic material derived from a calcifying strain of *E. huxleyi*.

Earlier chemostat studies conducted with various strains of *E. Huxleyi* revealed a general increase in cellular carbon contents (C-quotas) during P limitation, irrespective of CO_2 and temperature conditions (Fritz and Balch, 1996; Leonardos and Geider, 2005; Paasche, 1998; Riegman et al., 2000). For P-limited conditions at growth rates between 0.14 and 0.99 d^{-1}, C-quotas in a range of ~1–2 pmol $cell^{-1}$ were determined. Nutrient and growth conditions applied during this study to *E. huxleyi* (PML B 92/11) generally led to higher cell quotas for C of up to 2.7 pmol $cell^{-1}$, clearly decoupled from cell quotas for N and P (Table 2). For P, cell quotas for *E. huxleyi* grown under P limitation were shown to vary within 2.6 and 3.7 fmol $cell^{-1}$ (Riegman et al., 2000; Shaked et al., 2006). Riegman et al. (2000) determined a constant minimum P-quota of 2.6 fmol $cell^{-1}$ at growth rates of $D = 0.29$ and $D = 0.14$ d^{-1} and a pH of 8.0 during an earlier chemostat study with *E. huxleyi* (strain L) (Riegman et al., 2000). This value is in close relation to those we determined at similar growth rates for the 300-14 and 550-14 cultures, i.e. 2.70–3.09 fmol P $cell^{-1}$, but higher than the P-quota determined for the 900-18 culture; i.e. a minimum of 2.19 fmol P cell at 0.1 d^{-1} (Table 2). The lower P-quota in high CO_2 cells has to be reasoned by the higher cell density that was reached at elevated CO_2 and temperature while grown on identical nutrient supply. After the steady state cell yield was established, cell densities remained constant until the end of the experiment in all cultures. Thus, cells of all cultures maintained the capability to divide at identical rates, irrespective of differences in cell quotas for P. This suggests a large plasticity of the P-quota for *E. huxleyi* and also points to a decreased P demand of *E. huxleyi* under a combined rise in CO_2 and temperature (Table 2 and Fig. 7). A possible explanation for the low P-quotas of the greenhouse cells determined during our study might be a combined effect of P limitation and elevated CO_2 on the carbon concentrating mechanism (CCM) of *E. huxleyi*. Due to its low affinity for inorganic carbon and a low efficient CCM, *E. huxleyi* has been suggested to be carbon-limited in the present day ocean (Nielsen, 1995; Paasche, 1964; Rost and Riebesell, 2004; Rost et al., 2003). Carbon acquisition by CCM requires P to produce ATP providing energy for active transport processes. CCMs are therefore hypothesised to be down-regulated in algae grown under P limitation (Beardall and Giordano, 2002; Giordano et al., 2005) as shown for the green algae *Chlorella emersonii* (Beardall et al., 2005). During our experiment however, the increase in pCO_2 itself could have minimised the need of carbon concentration and might have led to a down-regulation of the energy efficient CCM. This possibly induced a lower P demand for *E. huxleyi* while grown at elevated CO_2.

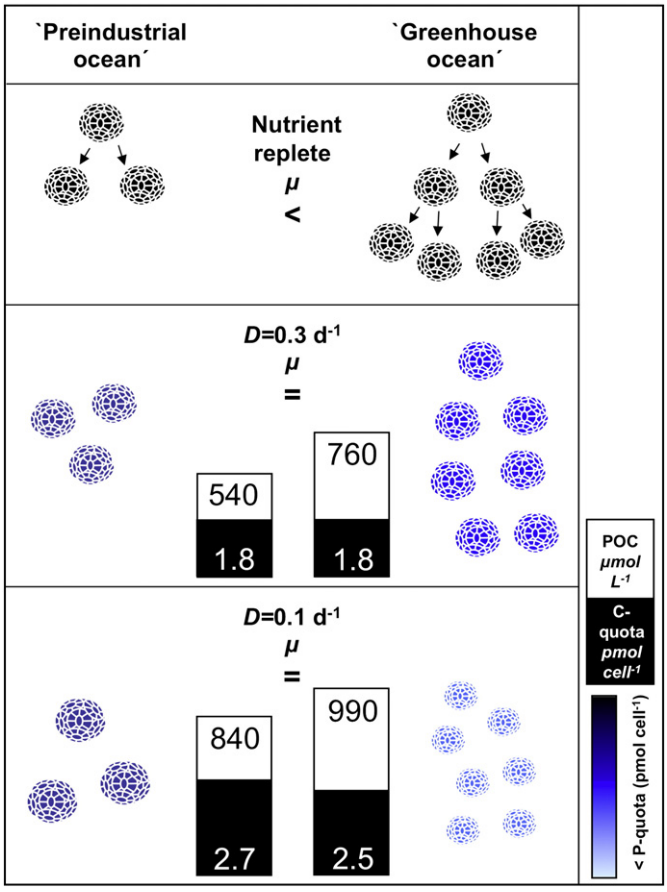

Fig. 7. Schematic drawing of the three growth stages during the *Emiliania huxleyi* experiment. Upper panel: *Bloom development* during the nutrient replete batch phase; Growth rates (μ) are significantly higher at 'greenhouse ocean' conditions compared to 'Pre-industrial' conditions. A higher cell density is reached on identical nutrient supply. Middle panel: Growth rates of both cultures adapt to the dilution rate (D) of 0.3 d^{-1}. Higher cell densities under greenhouse conditions are sustained on lower cell quota for phosphorous (P-quota). Significantly higher POC concentrations are produced at 'Greenhouse-conditions', while cell quotas for carbon (C-quota) are similar in both cultures. Lower panel: Growth rates of both cultures adapt to the dilution rate (D) of 0.1 d^{-1}. Higher cell densities at greenhouse conditions are sustained while P-quota probably fell below a critical value resulting in lower C-quota and cell volumes. Due to higher cell densities, POC concentrations (μmol L^{-1}) at 'Greenhouse-conditions' still exceed those produced at 'Pre-industrial-conditions'.

Nutrient limiting conditions were suggested to induce large variability concerning the C:N:P stoichiometry of algal biomass (Geider and LaRoche, 2002). Low growth rates applied during our study revealed an extended plasticity concerning a minimum P-quota for growth at high CO_2 conditions. Therefore a higher production of carbon rich biomass by *E. huxleyi* (PML B92/11) is to be expected, while grown under P-limited, greenhouse conditions. Throughout the experiment, highest POC (μmol L^{-1}), accompanied by highest molar POC:POP ratios, were determined in the 900-18 culture. Compared to POC:POP ratios of 400 (Leonardos and Geider, 2005) and ~490 (Riegman et al., 2000) determined for *E. huxleyi* under P limitation, maximum ratios of 1142 determined during our experiment more than doubled findings from other studies and the Redfield ratio of 106 by far. For bloom development in natural oligotrophic systems in the greenhouse ocean, results indicate accelerated growth and higher cell yield during a faster and extended bloom along with high concentrations of POC.

Earlier studies investigated the same *E. huxleyi* strain used here (PML B92/11) under nutrient-replete conditions at elevated CO_2 (Riebesell et al., 2000) or temperature (Langer et al., 2007). In both, a rise in CO_2 and temperature were shown to induce a positive response on POC production. Data presented here, however, demonstrate that cellular POC production remains unaffected by increased CO_2 and temperature under P-limitation (Fig. 6). Under enhanced P-stress at 0.1 d^{-1} cellular POC production even decreased with increasing CO_2 and temperature (Table 2 and Fig. 7). For nitrate-limited conditions, a similar decrease in cellular POC production at elevated CO_2 was reported earlier for *E. huxleyi* strain TW1 (Sciandra et al., 2003). Findings of both studies might indicate a general decrease of cellular POC production under nutrient depletion in the greenhouse ocean. However, the minimum P-value given by Riegman et al. (2000) for P-limited growth is the lowest P-quota for *E. huxleyi* reported so far. Hence, the P quota determined during our experiment probably fell below a critical value at 0.1 d^{-1}. Responses determined for C-quotas and cell sizes might therefore rather be reasoned by excessive P limitation than by elevated CO_2 and temperature (Fig. 7).

Cell volume of *E. huxleyi* was shown to increase with P limitation associated with an increase in C-quotas (Riegman et al., 2000). In our study, this observation does not hold for high-CO_2-cultures, since reduced cell volume was accompanied by an increase in cell normalised C after changing *D* from 0.3 d^{-1} to 0.1 d^{-1} (Table 2). This might be explained by an alternate source of POC, i.e. the abiotic formation of transparent exopolymer particles (TEP) in addition to POC derived from photosynthetic carbon assimilation by the cell. Carbon overconsumption is suggested to be accompanied by the release of dissolved organic compounds, especially under nutrient limited conditions (Banse, 1994; Engel et al., 2002; Myklestad et al., 1972). If exudates are not subject to bacterial degradation for example they might join the particulate carbon pool by the formation of carbon rich gel-particles like TEP (Engel et al., 2004). TEPs were shown to be related to rising CO_2 (Engel, 2002). Since TEPs are also retained on the filters during sampling of POC, *TEP–POC* is usually included in POC analysis for this methodical reason. The higher C-quota for cells of a smaller size might therefore either be explained by an overestimation of cell normalised POC due to the presence of TEP, by more POC per volume cell, or both (Table 2).

For *E. huxleyi* (PML B92/11), reduced PIC along with increased POC was reported earlier for high CO_2 treatment under nutrient replete conditions (Riebesell et al., 2000; Zondervan et al., 2001). Resulting lower PIC:POC ratios at high CO_2 conditions suggest higher export of organic matter to the ocean depth combined with a reduced release of CO_2 to the atmosphere providing a negative feedback to rising CO_2. In our study, Ω calcite was partly undersaturated and may have impaired net calcite production (Table 3). However, the decrease in PIC:POC ratios determined at the lower growth rate was due to higher POC since PIC remained unaffected (Table 2).

Combined effects of global change on *E. huxleyi*, a bloom-forming, cosmopolitan species, strongly affect the Redfield ratio that provides the basis for calculations of productivity and export of particulate organic matter in the ocean (Eppley and Peterson, 1979; Redfield et al., 1963). Overall, results obtained by this acidification and warming study indicate an even extended ability of *E. huxleyi* (PML B92/11) to grow with low P-quotas and produce carbon-rich biomass under greenhouse conditions. In nutrient limited situations or regions in the greenhouse ocean, the steep rise in POC:PON:POP ratios potentially increases the carbon export to the ocean depth.

Acknowledgements

We thank the AWI-workshop-team of Erich Dunker for technical support, Klaus-Uwe Richter for helpful discussions on the CO_2 aeration system and Christiane Lorenzen for assistance during the C/N-analysis. Judith Piontek and Gerald Langer are gratefully acknowledged for supportive discussions improving this manuscript. This research was supported by the Helmholtz Association contract no HZ-NG-102 and contributes to the Belgian Federal Science Policy Office PEACE project (contract no. SD/CS/03A/B). A.V. Borges is a research associate at the F.R.S.-F.N.R.S. This work has also been supported by the "European Project on Ocean Acidification" (EPOCA) which received funding from the European Community's Seventh Framework Programme (FP7/2007-2013) under grant agreement no. 211384. **[SS]**

References

Banse, K., 1994. Uptake of inorganic carbon and nitrate by marine plankton and the Redfield ratio. Global Biogeochem. Cycles 8, 81–84.
Barcelos e Ramos, J., Müller, M.N., Riebesell, U., 2010. Short-term response of the coccolithophore *Emiliania huxleyi* to an abrupt change in seawater carbon dioxide concentrations. Biogeosciences 7, 177–186.
Beardall, J., Giordano, M., 2002. Ecological implications of microalgal and cyanobacterial CO_2 concentrating mechanisms, and their regulation. Functional Plant Biology 29, 335–347.
Beardall, J., Roberts, S., Raven, J.A., 2005. Regulation of inorganic carbon acquisition by phosphorus limitation in the green alga *Chlorella emersonii*, pp. 859–864.
Berry, L., Taylor, A.R., Lucken, U., Ryan, K.P., Brownlee, C., 2002. Calcification and inorganic carbon acquisition in coccolithophores. Functional Plant Biology 29, 289–299.
Boyd, P.W., Doney, S.C., 2002. Modelling regional responses by marine pelagic ecosystems to global change. Geophys. Res. Lett. 29, 1806.
Caldeira, K., Wickett, M.E., 2003. Anthropogenic carbon and ocean pH. Nature 425, 365-365.
Caperon, J., 1968. Population growth response of *Isochrysis galbana* to nitrate variation at limiting concentrations. Ecology 49, 866–872.
Delille, B., Harlay, J., Zondervan, I., Jacquet, S., Chou, L., Wollast, R., Bellerby, R.G.J., Frankignoulle, M., Borges, A.V., Riebesell, U., Gattuso, J.P., 2005. Response of primary production and calcification to changes of pCO_2 during experimental blooms of the coccolithophorid *Emiliania huxleyi*. Global Biogeochemical Cycles 19, GB2023.
Dickson, A., 2010. The carbon dioxide system in sea water: equilibrium chemistry and measurements. In: Riebesell, U., Fabry, V.J., Hansson, L., Gattuso, J.-P. (Eds.), Guide to best practices for ocean acidification research and data reporting. Publications Office of the European Union, Luxembourg, p. 260.
Dickson, A.G., Millero, F.J., 1987. A comparison of the equilibrium constants for the dissociation of carbonic acid in seawater media. Deep Sea Research Part A. Oceanographic Research Papers 34, 1733–1743.
Dickson, A.G., Wesolowski, D.J., Palmer, D.A., Mesmer, R.E., 1990. Dissociation constant of bisulfate ion in aqueous sodium chloride solutions to 250 °C. J. Phys. Chem. 94, 7978–7985.
Droop, M.R., 1968. Vitamin B12 and Marine Ecology. IV. The kinetics of uptake, growth and inhibition in *Monochrysis lutheri*. Journal of the Marine Biological Association of the UK 48, 689–733.
Egge, J.K., Thingstad, T.F., Larsen, A., Engel, A., Wohlers, J., Bellerby, R.G.J., Riebesell, U., 2009. Primary production during nutrient-induced blooms at elevated CO_2 concentrations. Biogeosciences 6, 877–885.
Engel, A., 2002. Direct relationship between CO_2 uptake and transparent exopolymer particles production in natural phytoplankton. Journal of Plankton Research 24, 49–53.
Engel, A., Goldthwait, S., Passow, U., Alldredge, A., 2002. Temporal decoupling of carbon and nitrogen dynamics in a mesocosm diatom bloom. Limnol. Oceanogr. 47, 753–761.
Engel, A., Thoms, S., Riebesell, U., Rochelle-Newall, E., Zondervan, I., 2004. Polysaccharide aggregation as a potential sink of marine dissolved organic carbon. Nature 428, 929–932.
Engel, A., Ramos, J.B.e., Geider, R., Hutchins, D., Lee, C., Rost, B., Röttgers, R., Thingstad, F., 2010. Organic and export production, element ratios. Measurements of CO_2 sensitive processes. in: Guide for Best Practices in Ocean Acidification Research and Data Reporting (eds.): Riebesell U, Fabry V and J-P Gattuso.
Engel, A., Zondervan, I., Aerts, K., Beaufort, L., Benthien, A., Chou, L., Delille, B., Gattuso, J.P., Harlay, J., Heemann, C., Hoffmann, L., Jacquet, S., Nejstgaard, J., Pizay, M.D., Rochelle-Newall, E., Schneider, U., Terbrueggen, A., Riebesell, U., 2005. Testing the direct effect of CO_2 concentration on a bloom of the coccolithophorid *Emiliania huxleyi* in mesocosm experiments. Limnol. Oceanogr. 50, 493–507.
Eppley, R.W., Peterson, B.J., 1979. Particulate organic matter flux and planktonic new production in the deep ocean. Nature 282, 677–680.
Fabry, V.J., 2008. Ocean science — marine calcifiers in a high-CO_2 ocean. Science 320, 1020–1022.
Feng, Y., Warner, M.E., Zhang, Y., Sun, J., Fu, F.X., Rose, J.M., Hutchins, D.A., 2008. Interactive effects of increased pCO_2, temperature and irradiance on the marine coccolithophore *Emiliania huxleyi* (Prymnesiophyceae). European Journal of Phycology 43, 87–98.
Fritz, J.J., 1999. Carbon fixation and coccolith detachment in the coccolithophore *Emiliania huxleyi* in nitrate-limited cyclostats. Mar. Biol. 133, 509–518.
Fritz, J.J., Balch, W.M., 1996. A light-limited continuous culture study of *Emiliania huxleyi*: determination of coccolith detachment and its relevance to cell sinking. Journal of Experimental Marine Biology and Ecology 207, 127–147.
Gattuso, J.-P., Gao, K., Lee, K., Rost, B., Schulz, K., 2010. Approaches and tools to manipulate the carbonate chemistry. In: Riebesell, U., Fabry, V.J., Hansson, L., Gattuso, J.-P.

(Eds.), Guide to best practices for ocean acidification research and data reporting. Publications Office of the European Union, Luxembourg, p. 260.
Gattuso, J.P., Buddemeier, R.W., 2000. Ocean biogeochemistry — calcification and CO_2. Nature 407, 311–313.
Geider, R.J., LaRoche, J., 2002. Redfield revisited: variability of C:N:P in marine microalgae and its biochemical basis. European Journal of Phycology 37, 1–17.
Giordano, M., Beardall, J., Raven, J.A., 2005. CO_2 concentrating mechanisms in algae: mechanisms, environmental modulation, and evolution. Annual Plant Biology 56, 99–131.
Gran, G., 1952. Determination of the equivalence point in potentiometric titrations of seawater with hydrochloric acid. Oceanology Acta 5, 209–218.
Grasshoff, K., Kremeling, K., Ehrhardt, M., 1999. Methods of Seawater Analysis; Third, Completely Revised and Extended Edition. Wiley-VHC.
Guillard, R.R.L., Ryther, J.H., 1962. Studies of marine planktonic diatoms. I. Cyclotella nana Hustedt and Detonula confervacea Cleve. Canadian Journal of Microbiology 8, 229–239.
Hoppe, C., Langer, G., Rokitta, S., Wolf-Gladrow, D., Rost, B., 2010. On CO_2 pertubation experiments: over-determination of carbonate chemistry reveals inconsistencies. Biogeosciences Discussions 7, 1707–1726.
Houghton, J.T., Ding, Y., Griggs, D.J., Noguer, M., Van der Linden, P.J., Dai, X., Maskell, K., Johnson, C.A., 2001. Climate Change 2001: The Scientific Basis: Contribution of Working Group I to the Third Assessment Report of the Intergovernmental Panel of Climate Change.
Hutchins, D.A., Pustizzi, F., Hare, C.E., DiTullio, G.R., 2003. A shipboard natural community continuous culture system for ecologically relevant low-level nutrient enrichment experiments. Limnology and Oceanography-Methods 1, 82–91.
Iglesias-Rodriguez, M.D., Halloran, P.R., Rickaby, R.E.M., Hall, I.R., Colmenero-Hidalgo, E., Gittins, J.R., Green, D.R.H., Tyrrell, T., Gibbs, S.J., von Dassow, P., Rehm, E., Armbrust, E.V., Boessenkool, K.P., 2008. Phytoplankton calcification in a high-CO_2 world. Science 320, 336–340.
Koeve, W., Kim, H.-C., Lee, K., Oschlies, A., 2011. Potential impact of DOC accumulation on fCO_2 and carbonate ion computations in ocean acidification experiments. Biogeosciences Discussions 8, 3797–3827.
Koroleff, F., Grasshof, K., 1983. Determination of nutrients. In: Grasshof, K., Erhardt, M., Kremling, K. (Eds.), Methods of Seawater Analyses. Weinheim, Verlag Chemie, pp. 125–188.
Langer, G., Nehrke, G., Probert, I., Ly, J., Ziveri, P., 2009. Strain-specific responses of *Emiliania huxleyi* to changing seawater carbonate chemistry. Biogeosciences 6, 2637–2646.
Langer, G., Gussone, N., Nehrke, G., Riebesell, U., Eisenhauer, A., Thoms, S., 2007. Calcium isotope fractionation during coccolith formation in *Emiliania huxleyi*: Independence of growth and calcification rate. Geochemistry Geophysics Geosystems 8.
Langer, G., Geisen, M., Baumann, K.H., Klas, J., Riebesell, U., Thoms, S., Young, J.R., 2006. Species-specific responses of calcifying algae to changing seawater carbonate chemistry. Geochemistry Geophysics Geosystems 7.
LaRoche, J., Rost, B., Engel, A., 2010. Bioassays, batch culture and chemostat experimentation. In: Riebesell, U., Fabry, V.J., Hansson, L., Gattuso, J.-P. (Eds.), Guide to Best Practices for Ocean Acidification Research and Data Reporting. Publications Office of the European Union, Luxembourg, p. 260.
Leonardos, N., Geider, R.J., 2005. Elevated atmospheric carbon dioxide increases organic carbon fixation by *Emiliania huxleyi* (Haptophyta), under nutrient-limited high-light conditions. J. Phycol. 41, 1196–1203.
Lewis, E., Wallace, D., 1998. Program Developed for CO_2 System Calculations. ORNL/CDIAC-105, Carbon Dioxide Information Analysis Center, Oak Ridge National Laboratory, U.S. Department of Energy, Oak Ridge, Tennessee.
Meehl, G., Stocker, T., Collins, W., Friedlingstein, P., Gaye, A., Gregory, J., Kitoh, A., Knutti, R., Murphy, J., Noda, A., Raper, S., Watterson, I., Weaver, A., Zhao, Z.-C., 2007. Global Climate Projections. In: Climate Change 2007: The Physical Science Basis. Contribution of Working Group I to the Fourth Assessment Report of the Intergovernmental Panel on Climate Change In: Solomon, S., D. Qin, M. Manning, Z. Chen, M. Marquis, K.B. Averyt, M. Tignor and H.L. Miller (eds.) (Ed.).
Mehrbach, C., Culberso, Ch., Hawley, J.E., Pytkowic, Rm., 1973. Measurement of apparent dissociation-constants of carbonic-acid in seawater at atmospheric pressure. Limnol. Oceanogr. 18, 897–907.
Millero, F.J., 1995. Thermodynamics of the carbon-dioxide sysetm in the ocean. Geochimica Et Cosmochimica Acta 59, 661–677.
Monod, J., 1950. La technique de culture continue: theorie et applications. Ann. I. Pasteur Paris 79, 390.
Mucci, A., 1983. The solubility of calcite and aragonite in seawater at various salinities, temperature and one atmosphere total pressure. Am. J. Sci. 283, 780–799.
Müller, M.N., Schulz, K.G., Riebesell, U., 2010. Effects of long-term high CO2 exposure on two species of coccolithophores. Biogeosciences 7, 1109–1116.
Myklestad, S., Haug, A., Larsen, B., 1972. Production of carbohydrates by the marine diatom *Chaetoceros affinis* var Willei (Gran) In Hustedt II: preliminary investigation of the extracellular polysaccharide. Journal of Experimental Marine Biology and Ecology 9, 137–144.
Nielsen, M.V., 1995. Photosynthetic characteristics of the coccolithophorid *Emiliania huxleyi* (Prymnesiophyceae) exposed to elevated concentrations of dissolved inorganic carbon. J. Phycol. 31, 715–719.
Novick, A., Szilard, L., 1950. Description of the Chemostat. Science 112, 715–716.
Paasche, E., 1964. A tracer study of the inorganic carbon uptake during coccolith formation and photosynthesis in the coccolithophorid *Coccolithus huxleyi*. Physiology Plantarum Supplement 3, 1–82.
Paasche, E., 1998. Roles of nitrogen and phosphorus in coccolith formation in *Emiliania huxleyi* (Prymnesiophyceae). European Journal of Phycology 33, 33–42.
Paasche, E., 2002. A review of the coccolithophorid *Emiliania huxleyi* (Prymnesiophyceae), with particular reference to growth, coccolith formation, and calcification-photosynthesis interactions. Phycologia 40, 503–529.
Raupach, M.R., Marland, G., Ciais, P., Le Quere, C., Canadell, J.G., Klepper, G., Field, C.B., 2007. Global and regional drivers of accelerating CO_2 emissions. Proc. Natl. Acad. Sci. U. S. A. 104, 10288–10293.
Raven, J., Caldeira, K., Elderfield, H., Hoegh-Guldberg, O., Liss, P., Riebesell, U., Shepherd, J., Turley, C., Watson, A., 2005. Ocean Acidification Due to Increasing Atmospheric Carbon Dioxide. The Royal Society, London, UK.
Redfield, A.C., Ketchum, B.M., Richards, F.A., 1963. The influence of organism on the composition of seawater. In: Hill, M.N. (Ed.), The sea. Wiley, pp. 26–77.
Riebesell, U., Fabry, V., Hansson, L., Gattuso, J.-P., 2010. Guide to Best Practices in Ocean Acidification Research and Data Reporting.
Riebesell, U., Zondervan, I., Rost, B., Tortell, P.D., Zeebe, R.E., Morel, F.M.M., 2000. Reduced calcification of marine plankton in response to increased atmospheric CO_2. Nature 407, 364–367.
Riebesell, U., Schulz, K.G., Bellerby, R.G.J., Botros, M., Fritsche, P., Meyerhofer, M., Neill, C., Nondal, G., Oschlies, A., Wohlers, J., Zollner, E., 2007. Enhanced biological carbon consumption in a high CO_2 ocean. Nature 450 (545-U510).
Riegman, R., Stolte, W., Noordeloos, A.A.M., Slezak, D., 2000. Nutrient uptake and alkaline phosphatase (ec 3:1:3:1) activity of *Emiliania huxleyi* (Prymnesiophyceae) during growth under N and P limitation in continuous cultures. J. Phycol. 36, 87–96.
Rost, B., Riebesell, U., 2004. Coccolithophores and the biological pump: responses to environmental changes. In: Thierstein, H.R., Young, J.R. (Eds.), Coccolithophores. From Molecular Processes to Global Impact, pp. 99–127.
Rost, B., Zondervan, I., Wolf-Gladrow, D., 2008. Sensitivity of phytoplankton to future changes in ocean carbonate chemistry: current knowledge, contradictions and research directions. Mar. Ecol. Prog. Ser. 373, 227–237.
Rost, B., Riebesell, U., Burkhardt, S., Sultemeyer, D., 2003. Carbon acquisition of bloom-forming marine phytoplankton. Limnol. Oceanogr. 48, 55–67.
Sarmiento, J.L., Slater, R., Barber, R., Bopp, L., Doney, S.C., Hirst, A.C., Kleypas, J., Matear, R., Mikolajewicz, U., Monfray, P., Soldatov, V., Spall, S.A., Stouffer, R., 2004. Response of ocean ecosystems to climate warming. Global Biogeochem. Cycles 18, GB3003.
Schulz, K.G., Ramos, J.B.E., Zeebe, R.E., Riebesell, U., 2009. CO_2 perturbation experiments: similarities and differences between dissolved inorganic carbon and total alkalinity manipulations. Biogeosciences 6, 2145–2153.
Sciandra, A., Harlay, J., Lefèvre, D., Lemée, R., Rimmelin, P., Denis, M., Gattuso, J.-P., 2003. Response of the coccolithophorid *Emiliania huxleyi* to elevated pCO_2 under nitrate limitation. Mar. Ecol. Prog. Ser. 261, 111–122.
Shaked, Y., Xu, Y., Leblanc, K., Morel, F.M.M., 2006. Zinc availability and alkaline phosphatase activity in *Emiliania huxleyi*: implications for Zn-P co-limitation in the ocean. Limnol. Oceanogr. 51, 299–309.
Thierstein, H., Young, J.R., 2004. Coccolithophores; From Molecular Processes to Global Impact. Springer.
Toggweiler, J.R., 1993. Carbon overconsumption. Nature 363, 210–211.
Zeebe, R., Wolf-Gladrow, D., 2001. CO_2 in Seawater: Equilibrium, Kinetics. Isotopes, Amsterdam.
Zondervan, I., Rost, B., Riebesell, U., 2002. Effect of CO_2 concentration on the PIC/POC ratio in the coccolithophore *Emiliania huxleyi* grown under light-limiting conditions and different daylengths. Journal of Experimental Marine Biology and Ecology 272, 55–70.
Zondervan, I., Zeebe, R.E., Rost, B., Riebesell, U., 2001. Decreasing marine biogenic calcification: a negative feedback on rising atmospheric pCO(2). Global Biogeochem. Cycles 15, 507–516.